

Supporting Information for:

## High Tolerance to Iron Contamination in Lead Halide Perovskite Solar Cells

Jeremy R. Poindexter<sup>1</sup>, Robert L. Z. Hoye<sup>1,†</sup>, Lea Nienhaus<sup>1</sup>, Rachel C. Kurchin<sup>1</sup>, Ashley E. Morishige<sup>1</sup>, Erin Looney<sup>1</sup>, Anna Osherov<sup>1</sup>, Juan-Pablo Correa-Baena<sup>1</sup>, Barry Lai<sup>2</sup>, Vladimir Bulović<sup>1</sup>, Vladan Stevanović<sup>3,4</sup>, Mounqi G. Bawendi<sup>1</sup>, Tonio Buonassisi<sup>1</sup>

<sup>1</sup>*Massachusetts Institute of Technology, Cambridge, MA 02139*

<sup>2</sup>*Advanced Photon Source, Argonne National Laboratory, 9700 Cass Avenue, Argonne, IL 60439*

<sup>3</sup>*Colorado School of Mines, 1500 Illinois Street, Golden, CO 80401*

<sup>4</sup>*National Renewable Energy Laboratory, 15013 Denver West Parkway, Golden, CO 80401*

<sup>†</sup>current address: *Cavendish Laboratory, University of Cambridge, JJ Thomson Avenue CB3 0HE, UK*

### A. Film and device synthesis details

Solar cells were fabricated by making slight alterations from the recipes used by Lee *et al*<sup>1</sup>. 1”×1” fluorine-doped tin oxide (FTO) substrates (Thin Film Devices) with sheet resistances of  $15 \pm 3 \Omega/\square$  were cleaned in a heated (37–52 °C) ultrasonic bath for 5–9 min each in deionized water, acetone, ethanol, and isopropanol, dried with N<sub>2</sub>, and cleaned under oxygen plasma for 10 min at a pressure of –90 kPa (gauge). Sol-gel TiO<sub>2</sub> was prepared by dissolving 350 µL of titanium(IV) isopropoxide (0.24 M, Sigma-Aldrich, 99.999%) and 35 µL of hydrochloric acid (12 M) in 2.5 mL of ethanol, and the resulting solution was spin-coated onto cleaned substrates at 1500 rpm for 45 s (1500 rpm/s acceleration) inside a dry-air glovebox (relative humidity < 4%) to form a compact TiO<sub>2</sub> layer. Samples were then annealed in ambient air at 150 °C for 10 min, allowed to cool to room temperature, then heated to 350 °C over 30 min, to 540 °C for 1 h, cooled to 350 °C over 30 min, then allowed to cool overnight.

Perovskite precursor solutions were prepared in a nitrogen-filled glovebox by dissolving methylammonium iodide (Dyesol, ≥ 99%) and lead(II) chloride (Sigma-Aldrich, 99.999%) in a 3:1 molar ratio (2.27 / 0.76 M) and *N,N*-dimethylformamide (DMF, Sigma-Aldrich 99.8%) to form a 38 wt.% solution. Iron was incorporated by separately preparing a “base” iron(II) iodide (Sigma-Aldrich, 99.99%) solution (0.31 M) in DMF, which served as the 1000 ppm source. Solutions for the 1, 10, and 100 ppm samples were prepared by sequential dilution and each added to separate perovskite solutions, which ensured that the same amount of total DMF solvent remained in all solutions. The 1 at.% solution was prepared separately (using the same 38 wt% solution before any FeI<sub>2</sub> was added) since FeI<sub>2</sub> would not fully dissolve in DMF at concentrations much higher than 0.31 M. After the addition of FeI<sub>2</sub>, solutions were vortexed, mixed for ~60 min with a stir bar, and put through a 0.2 µm PTFE filter.

After preparation, perovskite solutions were spun onto the TiO<sub>2</sub>-covered substrates in the nitrogen-filled glovebox at 2000 rpm for 45 s (2000 rpm/s acceleration), allowed to dry for 30 min inside the nitrogen-filled glovebox while purging, then heated on a hot plate at 100 °C for 150 min.

To make solar cells, a solution of spiro-OMeTAD (2,2',7,7'-Tetrakis(N,N-di-p-methoxyphenylamino)-9,9'-spirobifluorene, 0.08 M, Lumtech, >99.5%) was prepared by dissolving spiro-OMeTAD powder in chlorobenzene, to which small amounts (45 and 10  $\mu$ L per mL of chlorobenzene, respectively) of 175 mg/mL bis(trifluoromethane) sulfonimide lithium salt (Sigma-Aldrich, 99.95%) in acetonitrile and 4-tert-butylpyridine (Sigma-Aldrich, 96%) were added. The spiro-OMeTAD solution was spun onto the substrates at 4000 rpm for 45 s (4000 rpm/s acceleration). Samples were exposed to oxygen overnight in a desiccator to increase conductivity prior to depositing 100 nm Au via thermal evaporation at 0.1–0.3 Å/s.

## B. Additional *J–V* data

### B1. *J–V* curves after 1.4 V pre-sweep bias

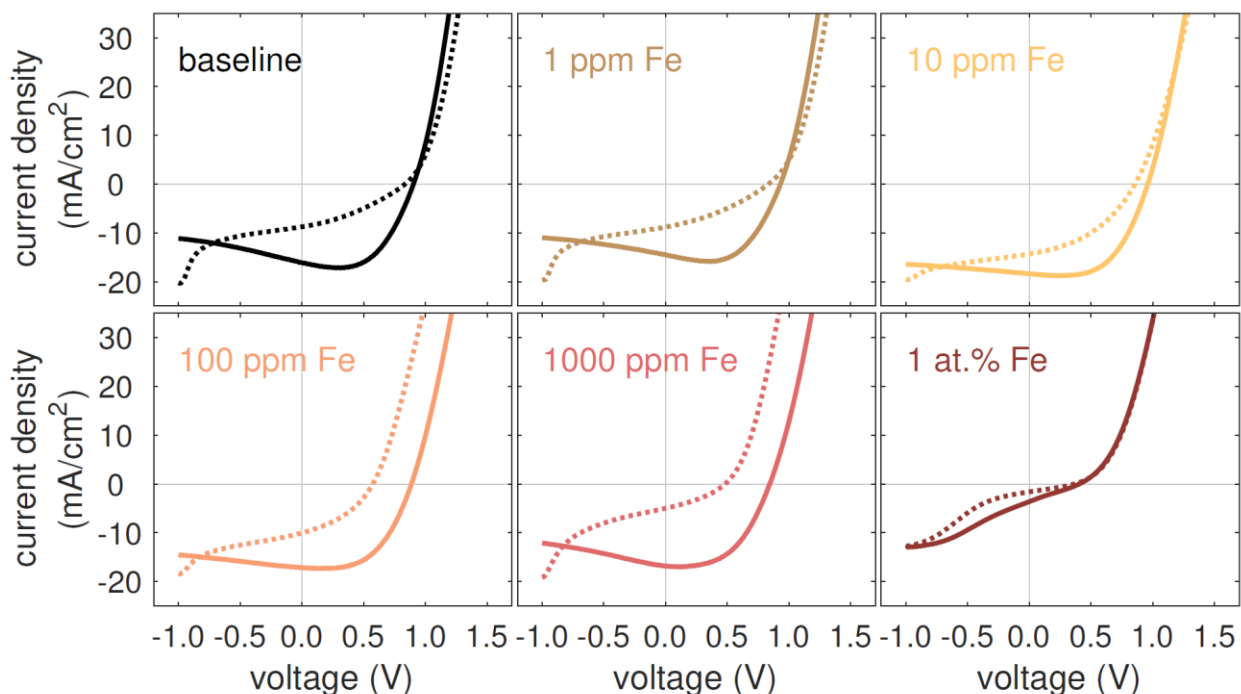


Figure S1. *J–V* sweeps taken after a 1.4 V pre-bias for 60 s in the dark in the reverse (solid lines) and forward (dotted lines) directions. Devices and scan sweep parameters (besides the pre-sweep bias) identical as in Figure 1.

## B2. $J$ - $V$ boxplot summary (forward sweeps)

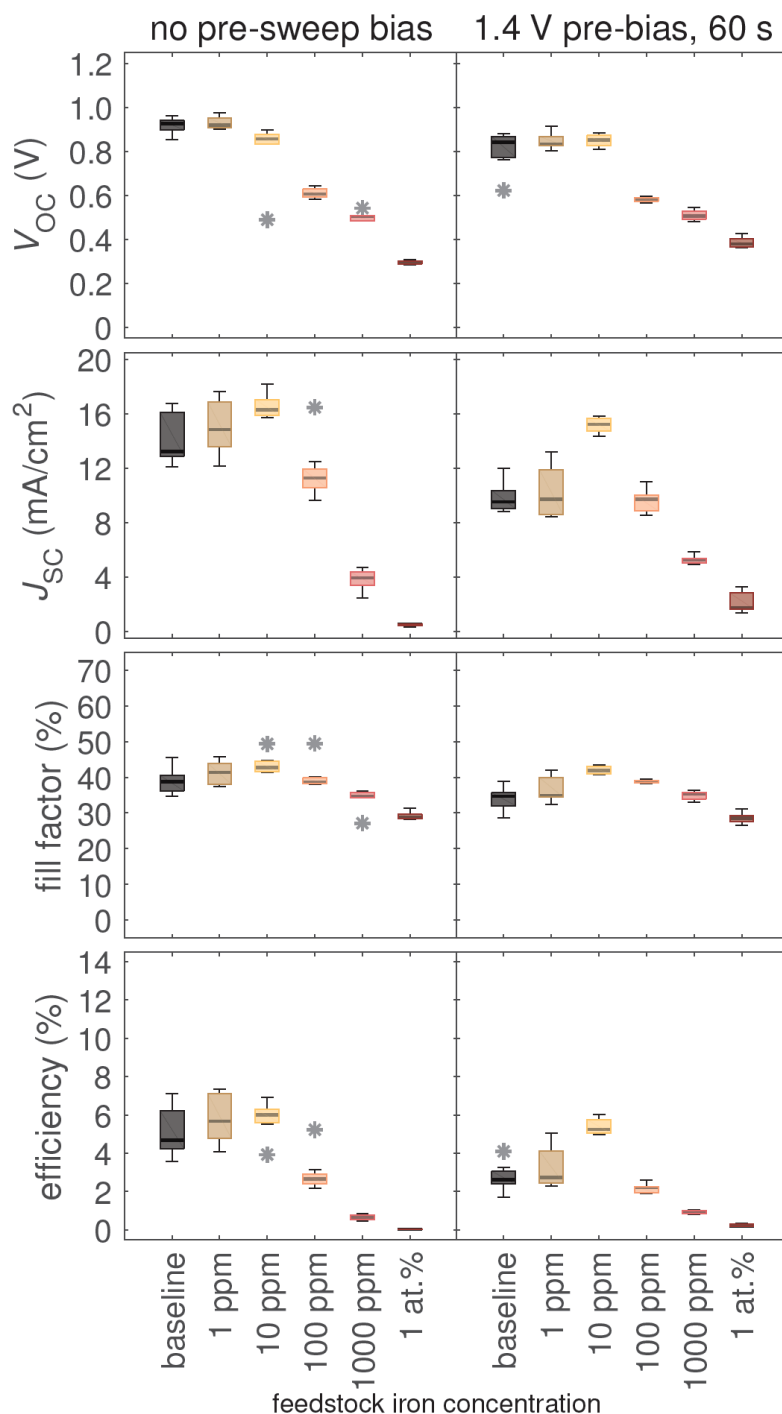


Figure S2. Boxplot summary of  $J$ - $V$  parameters for sweeps taken in the forward direction with (right column) and without (left column) a 1.4 V pre-sweep bias taken in the dark for 60 s. Box upper and lower bounds represent 75% and 25% percentile marks, respectively. Whiskers indicate data extrema up to 2.7 standard deviations away from mean. Asterisks represent outliers (more than 2.7 standard deviations away from mean).

## C. Structural characterization

### C1. Film morphology

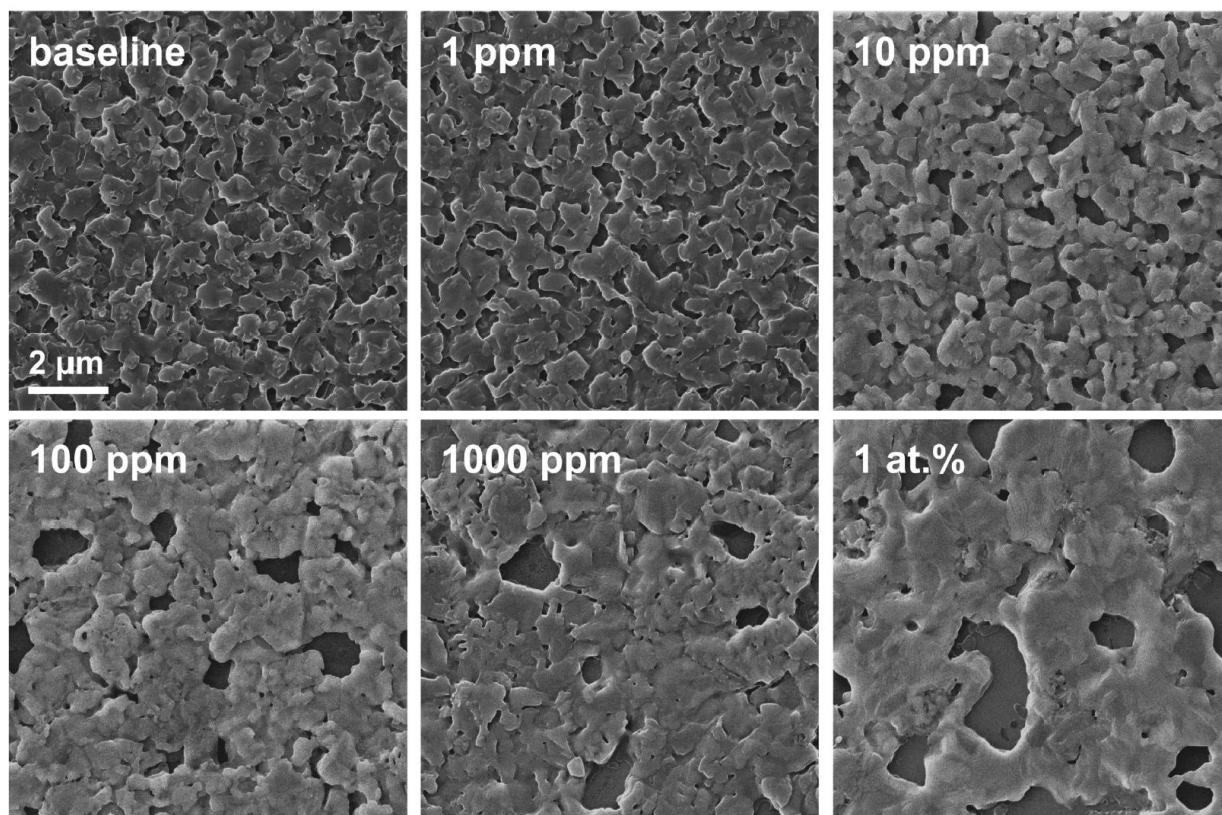


Figure S3. Helium-ion microscopy images of glass/TiO<sub>2</sub>/MAPbI<sub>3</sub> films collected on a Zeiss Orion Plus system. Scale bar applies to all images.

## C2. X-ray diffraction data

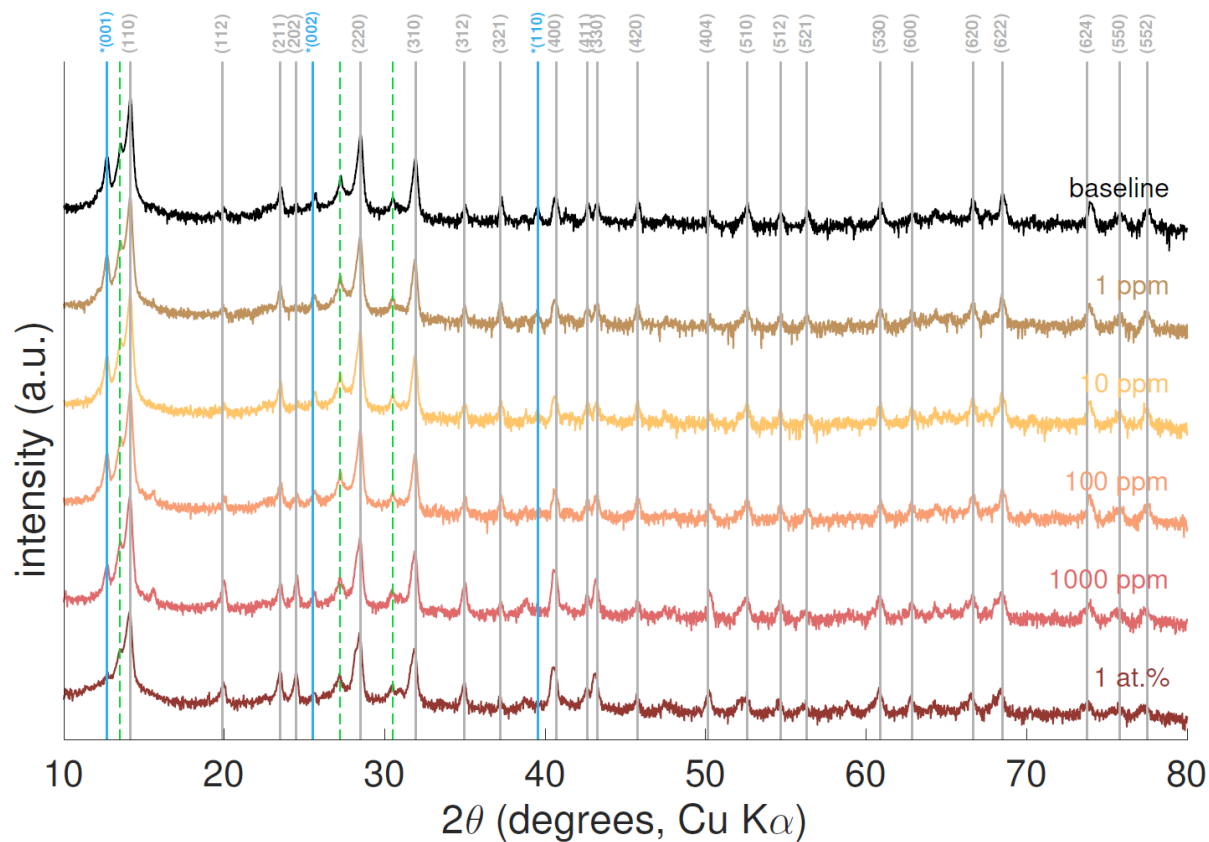


Figure S4. Semilog plot of X-ray diffraction measurements collected in grazing incidence mode (angle of incidence =  $0.5^\circ$ ) on glass/TiO<sub>2</sub>/MAPbI<sub>3</sub> films collected on a Rigaku SmartLab Multipurpose Diffractometer with parallel beam optics, a parametric slit analyzer, and a copper anode. Peaks corresponding to MAPbI<sub>3</sub> (solid gray lines) suggest the incorporation of iron does not induce large structural changes in the film. Some residual PbI<sub>2</sub> (solid blue lines with asterisks) is evident. Some residual peaks (dotted green lines) are due to tungsten  $L\alpha_1$  emission from the filament and occurs near the strongest MAPbI<sub>3</sub> peaks.

## D. Additional XPS plots

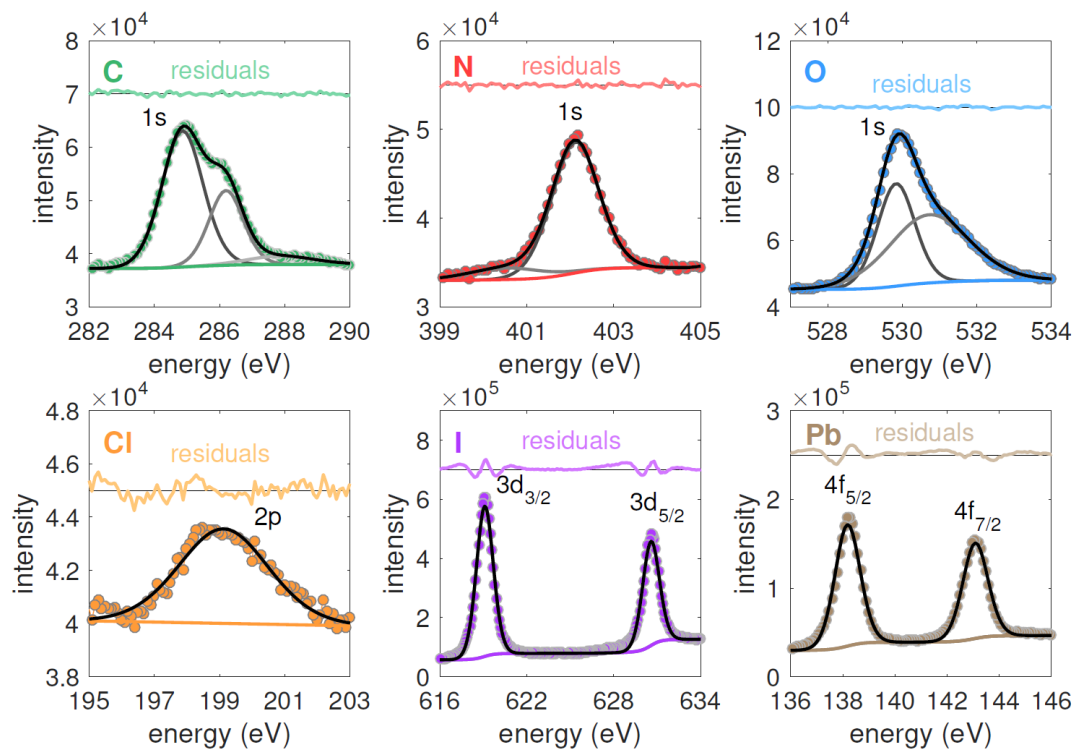


Figure S5. Additional XPS data of primary elements in MAPbI<sub>3</sub> with 1 at.% feedstock iron concentration showing experimental data (filled circles), background (darker colored lines), peak fits (black), and residuals (lighter colored lines).

## **E. Alternate device architecture: solar cell fabrication and *J–V* testing**

### **E1. Device synthesis recipe**

Following the structure described by Docampo *et al.*<sup>2</sup>, solar cells were fabricated on 12mm×12mm glass/ITO substrates (Thin Film Devices) with sheet resistances of 20  $\Omega/\square$  which were cleaned in an ultrasonic bath for 10 min each in acetone and isopropanol, then cleaned under oxygen plasma for 10 min. 35  $\mu\text{L}$  of poly(3,4-ethylenedioxythiophene) polystyrene sulfonate (PEDOT:PSS, Ossila) was spin-coated onto cleaned 1cm×1cm substrates, which were then spun for 4000 rpm at 30 s and annealed for 130 °C for 20 min in air.

Perovskite precursor solutions were prepared in a nitrogen-filled glovebox by weighing together methylammonium iodide (Dyesol,  $\geq 99\%$ ) and lead(II) acetate trihydrate (Sigma-Aldrich, 99.999%) in a 3:1 molar ratio (2.67 / 0.88 M) and dissolving them in DMF.  $\text{FeI}_2$  was incorporated similarly as for the FTO-based devices. Solutions were then mixed at 50 °C for 15 min with a stir bar and put through a 0.2  $\mu\text{m}$  PTFE filter.

After preparation, perovskite solutions were spun onto the PEDOT:PSS-covered substrates in a drybox by “hot casting”: substrates were heated to 85 °C, placed immediately onto the spincoater, and spun at 2000 rpm for 40 s. 35  $\mu\text{L}$  perovskite solution was warmed to 50 °C, then dispensed onto the middle of the substrate within the first 10 s of spinning. After spincoating, the sample was left to anneal at 85 °C for 20 min, then left inside the drybox for 4 h.

Phenyl- $\text{C}_{61}$ -butyric acid methyl ester (PCBM) solution was prepared by dissolving 20 mg/mL  $\text{PC}_{60}\text{BM}$  (nano-C,  $\geq 99.5\%$ ) in chlorobenzene in a vial, which was placed on a hot plate at 50 °C prior to spincoating. Substrates were spun at 1400 rpm for 40 s and 3000 rpm for 10 s, and 15  $\mu\text{L}$  of PCBM solution was deposited during the first 10 s of spinning. 20 nm Ca (0.1–0.2  $\text{\AA}/\text{s}$ ) and 80 nm Al (0.1  $\text{\AA}/\text{s}$  initially then up to 5  $\text{\AA}/\text{s}$ ) were then deposited via thermal evaporation. The devices were placed in a sealed nitrogen-filled tube and transferred to a nitrogen-filled glovebox for *J–V* measurements to prevent the Ca/Al electrodes from corroding in air.

## E2. $J$ - $V$ data

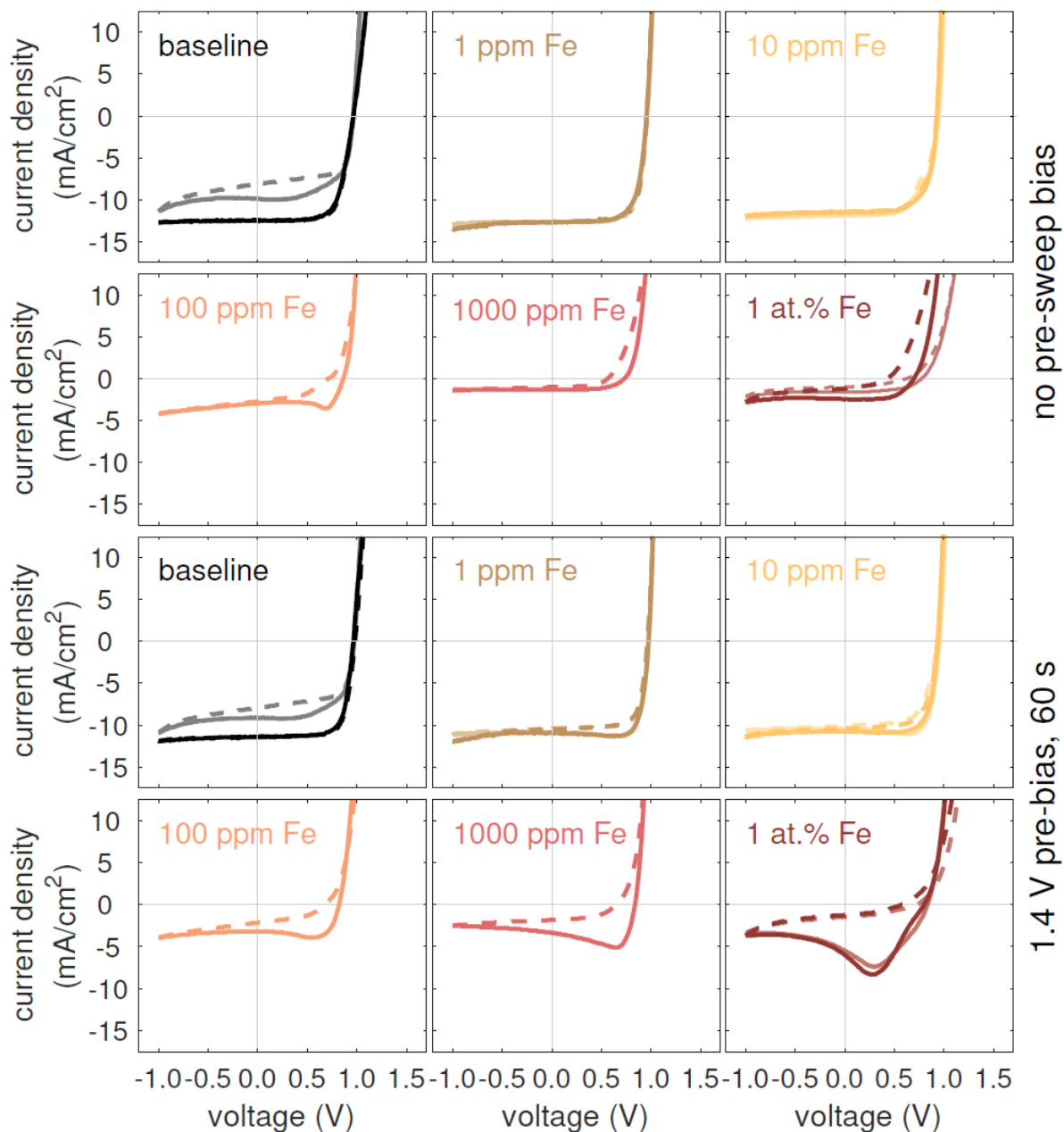


Figure S6.  $J$ - $V$  sweeps on alternate architecture in the reverse (solid lines) and forward (dotted lines) directions for no pre-sweep bias (top two rows) and a 1.4 V pre-sweep bias (bottom two rows). Taken on a Newport Oriel solar simulator (model 67005) with a scan speed of 0.1 V/s in each direction under 1-Sun illumination and a  $N_2$  ambient. For each sample, the plot shown is the device closest to the median efficiency of 4–6 devices. For the baseline, 1 ppm, 10 ppm, and 1 at.% plots, two median devices (one from each pair of samples) are plotted. The apparent “negative” shunt resistances for some devices are due to time-dependent charging effects caused by device hysteresis. Devices were masked with a metal aperture to obtain a measurement area of  $0.544 \text{ cm}^2$ .



### E3. $J$ - $V$ boxplot summary

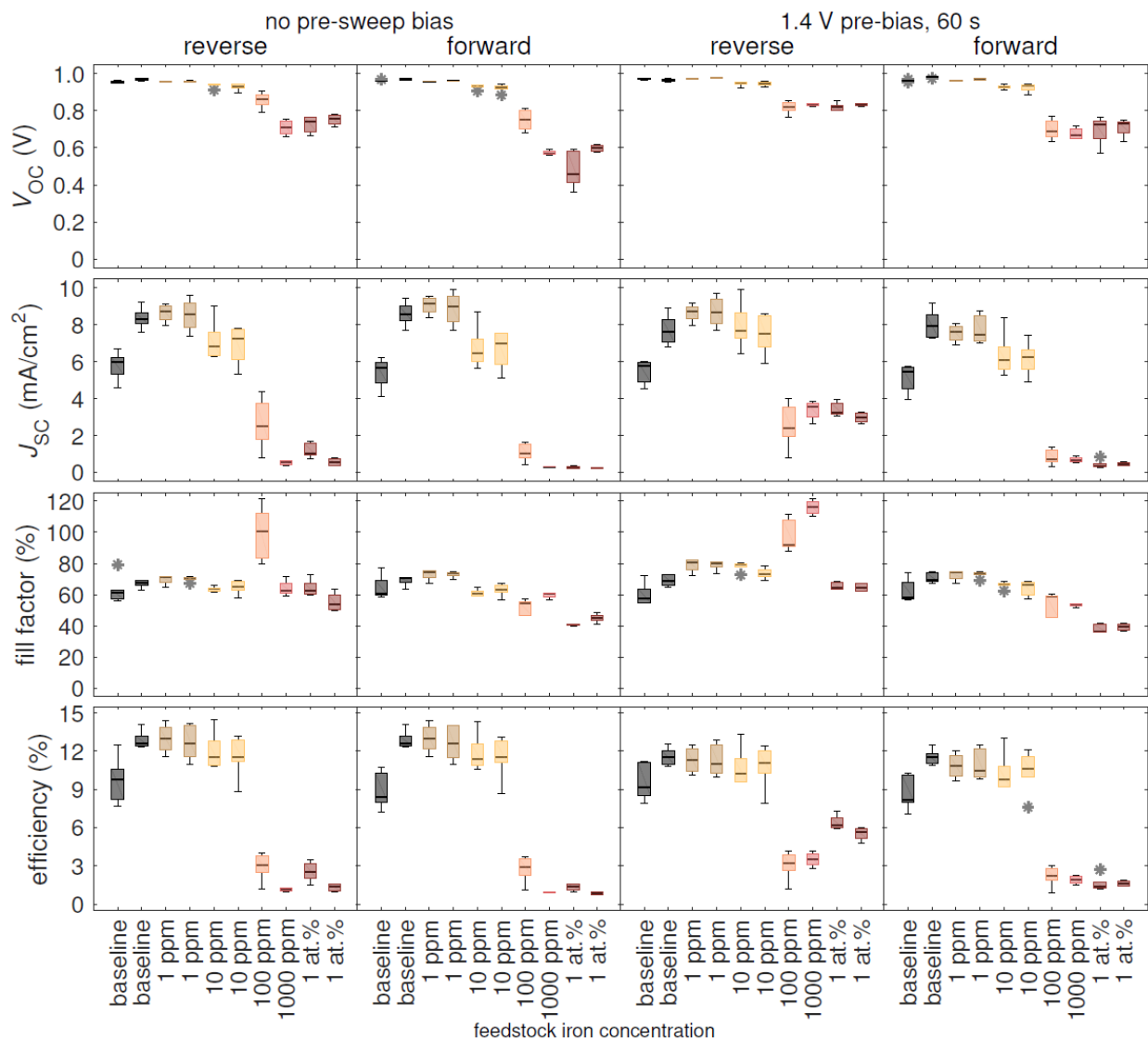


Figure S7. Boxplot summary of  $J$ - $V$  parameters on alternate architecture in the reverse (filled boxes) and forward (empty boxes) directions, both with (right two columns) and without (left two columns) a 1.4 V pre-sweep bias for 60 s. Box upper and lower bounds represent 75% and 25% percentile marks, respectively. Whiskers indicate data extrema up to 2.7 standard deviations away from mean. Asterisks represent outliers (more than 2.7 standard deviations away from mean). Ten out of twelve samples fabricated are shown; two were omitted due to poor repeatability. The fill factors exceeding 100% for some samples are due to the time-dependent  $J$ - $V$  response caused by device hysteresis.

## F. Film absorbance

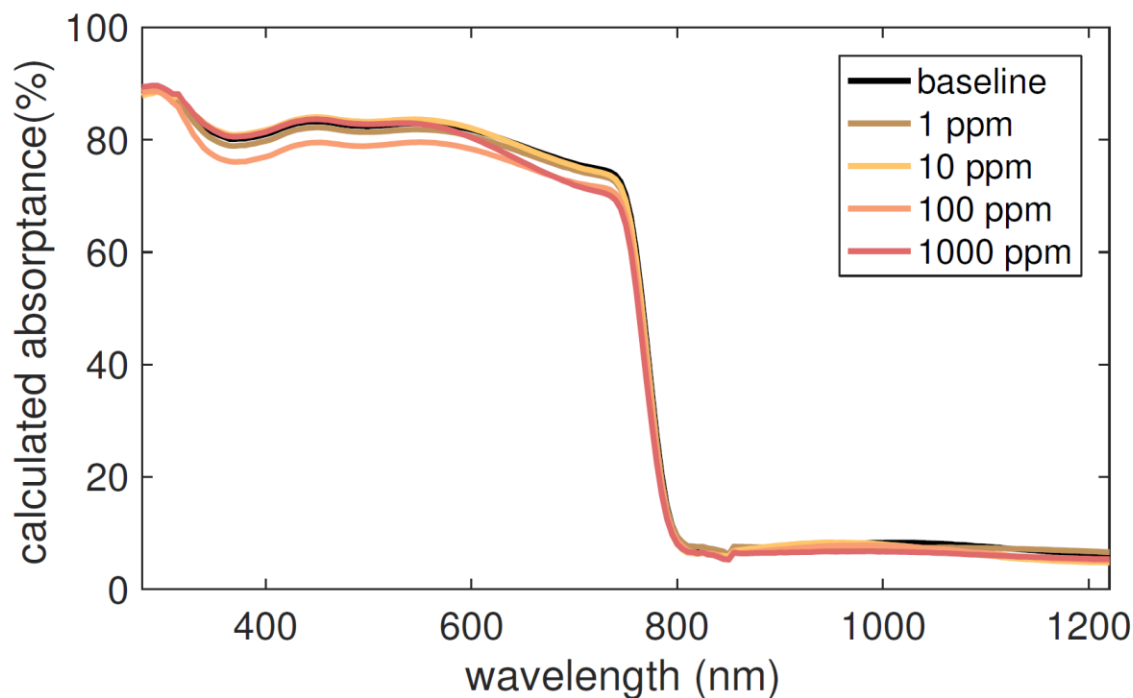


Figure S8. Film absorbance as calculated from  $1-T-R$ , where  $T$  and  $R$  are transmittance and reflectance, respectively, collected on a PerkinElmer Lambda 900 Spectrometer with 5 nm wavelength resolution. 0% and 100% baselines were collected using an internal attenuator and a Spectralon mirror, respectively. The small spike in the data at 860 nm is a minor artifact due to the changeover in detectors from InGaAs to a photomultiplier tube.

## References

- (1) Lee, M. M.; Teuscher, J.; Miyasaka, T.; Murakami, T. N.; Snaith, H. J. Efficient Hybrid Solar Cells Based on Meso-Superstructured Organometal Halide Perovskites. *Science* **2012**, *338*, 643–647.
- (2) Docampo, P.; Ball, J. M.; Darwich, M.; Eperon, G. E.; Snaith, H. J. Efficient Organometal Trihalide Perovskite Planar-Heterojunction Solar Cells on Flexible Polymer Substrates. *Nat. Commun.* **2013**, *4*, 2761.